



## Noncontact Group Delay Based Sensor for Metal Deformation and Crack Detection

Chen, Zhe; Lin, Xianqi; Yan, Yu Heng; Xiao, Feng; Khan, Muhammad Talha; Zhang, Shuai

*Published in:*  
I E E E Transactions on Industrial Electronics

*DOI (link to publication from Publisher):*  
[10.1109/TIE.2020.3008386](https://doi.org/10.1109/TIE.2020.3008386)

*Creative Commons License*  
Unspecified

*Publication date:*  
2021

*Document Version*  
Accepted author manuscript, peer reviewed version

[Link to publication from Aalborg University](#)

*Citation for published version (APA):*  
Chen, Z., Lin, X., Yan, Y. H., Xiao, F., Khan, M. T., & Zhang, S. (2021). Noncontact Group Delay Based Sensor for Metal Deformation and Crack Detection. *I E E E Transactions on Industrial Electronics*, 68(8), 7613-7619. [9141515]. <https://doi.org/10.1109/TIE.2020.3008386>

### General rights

Copyright and moral rights for the publications made accessible in the public portal are retained by the authors and/or other copyright owners and it is a condition of accessing publications that users recognise and abide by the legal requirements associated with these rights.

- Users may download and print one copy of any publication from the public portal for the purpose of private study or research.
- You may not further distribute the material or use it for any profit-making activity or commercial gain
- You may freely distribute the URL identifying the publication in the public portal -

### Take down policy

If you believe that this document breaches copyright please contact us at [vbn@aub.aau.dk](mailto:vbn@aub.aau.dk) providing details, and we will remove access to the work immediately and investigate your claim.

# Noncontact Group-Delay-Based Sensor for Metal Deformation and Crack Detection

Zhe Chen, Xian Qi Lin\*, *Senior Member, IEEE*, Yu Heng Yan,  
Feng Xiao, Muhammad Talha Khan, and Shuai Zhang, *Senior Member, IEEE*

**Abstract**—A millimeter-wave planar resonator sensor for the detection of deformation and crack in metal device with high precision and sensitivity is presented in this paper. The deformation and crack directly imply great damage in the industrial metal structures, which made the detection crucial in structural health monitoring (SHM). The main structure of the proposed sensor is based on the concept of multi-band electromagnetic induced transparency (EIT) effect. EIT effect is an interference quantum phenomenon which can be realized in microwave band by electromagnetic resonate structures. Multi-band EIT is actualized using serious of split-ring-resonators (SRR) coupling with each other to produce one wide stop band and four narrow pass band. The resonance frequencies of the SRRs are effected by variation of coupling amount between the SRRs and the part of metal device under test (DUT) that places close to the specific SRR. The orientation of metal deformation and crack is achieved by different frequency shifts of the four independent group delay peaks induced by multi-band EIT. Thus, the proposed sensor can orientate the deformation on the metal device with the precision of 1.3MHz/um.

**Index Terms**—Electromagnetic induced transparency, metal deformation sensor, metal crack sensor, split ring resonator.

## I. INTRODUCTION

STRUCTURAL health monitoring is a hot topic in aerospace, civil infrastructure, industrial production and other fields. At present, some engineering structures crack or deform due to overload or extreme environment, causing catastrophic disaster. For safety, these structures need to be regularly monitored for potential safety hazards. However, manual detection is very difficult, and requires significant costs in time and resources. There are many kinds of detection methods at present, such as fiber Bragg grating sensor technology [1], electroluminescent

strain sensor technology [2] and image-based crack detection particle filter technology [3]. However, most of the existing methods have relatively high costs and need to be closely attached to the surface of the structure or embedded in the structure [4], which may cause certain influence on the structure.

Noncontact and nondestructive sensing capability, multifunction, high precision, high sensitivity, and good penetration are some of the advantages that millimeter-wave sensors possess [5]. Recently, they are widely used in plenty of industrial applications, such as localization [6-8], gesture recognition [9], pipeline coating breaches detection [10-11] and metal crack characterization [12]. Metal components and containers are widely used in industrial procedure. The health of metal structure is important. So, the detection of the deformation and crack of the metal structure is very important. The sensor proposed in this paper can provide high precision orientation.

Although the implementation of the structures and the application scenarios vary, sensors work based on the shift of electrical parameters such as amplitude, phase and frequency. Group delay is a crucial parameter that relates to sensitivity and has been applied in fiber sensing and integrated optical refractometric sensing [13-15]. The pros of group-delay-based sensors consist of ultrahigh sensitivity and the ability of operating in time domain. Nair *et al.* designed a RFID humidity sensor using C-sections for group delay peak producing, the sensing is achieved by depositing the nanowires on the C-sections [16].

In this paper, the concept of Electromagnetic induced transparency (EIT) is adopted for the design of group-delay-based sensor. EIT effect is a destructive quantum interference effect that refers to the formation of a transmission window inside the absorption band of a three-level atomic media. It has been found out that many microwave resonant coupling structures can be configured to EIT-like effect [17-20]. EIT-like effect can be obtained by one resonator called “bright” which supports a broad adsorbing band and another resonator called “dark” that supports a narrow resonance coupling with each other. Generally, the bright mode exhibits a strong coupling to the radiation field, whereas the dark mode is excited by its coupling to the bright mode [21]. It can also be evoked in a single fano resonator consisting of asymmetric resonance structure [22]. These EIT-like structures can produce large group delay and high quality factor.

Manuscript received November 26, 2019; revised Mar 7, 2020 and May 29, 2020; accepted Jun 28, 2020. This work was supported by in part by National Natural Science Foundation of China (NSFC) under Grant No. 61571084 and U1966201, and in part by the Fundamental Research Funds for the Central Universities (FRFCU) under Grant No. ZYGX2019Z022 and XGBDFZ03.

Z. Chen, X.Q. Lin, Y.H. Yan, F. Xiao and M.T. Khan are with the School of Electronic Science and Engineering, University of Electronic Science and Technology of China, Chengdu 611731, China (Corresponding author: Xian Qi Lin, e-mail: xqlin@uestc.edu.cn).

S. Zhang is with the Antennas, Propagation and Millimeter-wave Systems (APMS) section, Department of Electronic Systems, Aalborg University, Aalborg, 9220, Denmark. (email: sz@es.aau.dk).

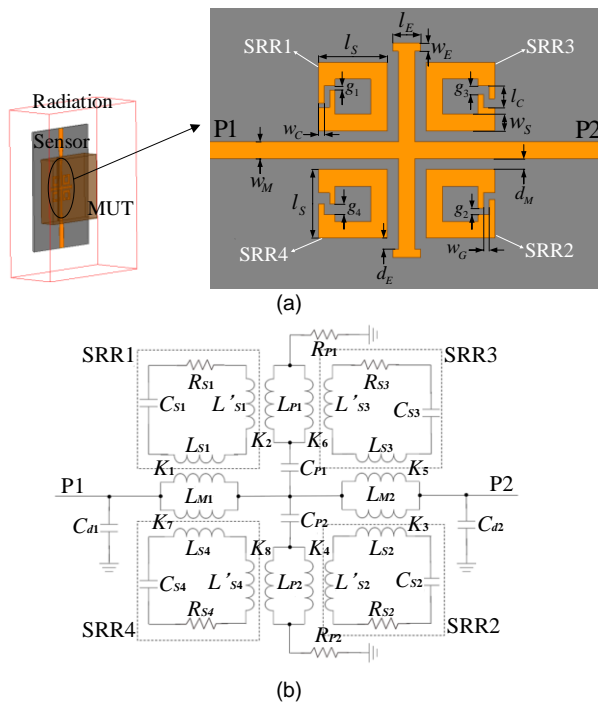


Fig. 1. Layout of the proposed multiband sensor.

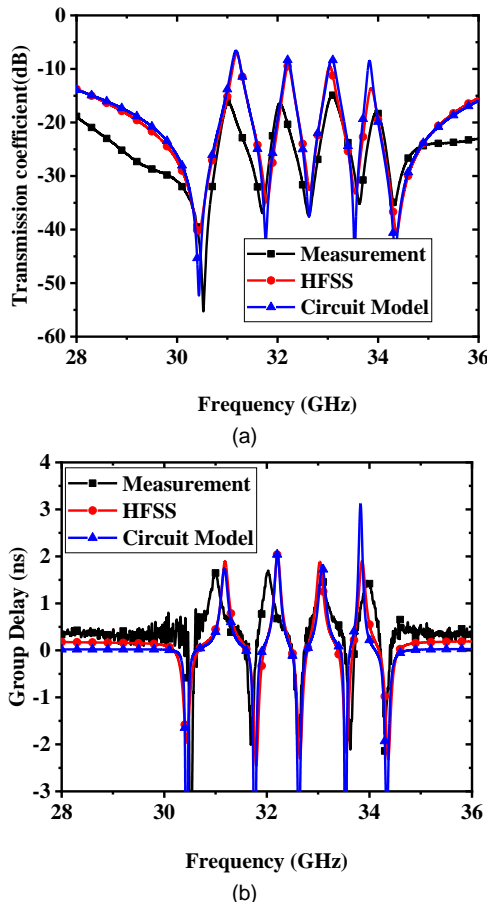


Fig. 2. Measurement, simulation and circuit model results of the multiband sensor.

Table 1 The parameters of the lumped components

$C_{d1}=336.15$ fF	$C_{d2}=259.79$ fF	$L_{M1}=267.85$ pH	$L_{M2}=25.39$ pH	$C_{P1}=0.01$ fF
$C_{P2}=0.1056$ fF	$L_{P1}=616.66$ nH	$L_{P2}=211.23$ nH	$R_{P1}=26.49$ mOhm	$R_{P2}=2.35$ Ohm
$C_{S1}=1.09$ fF	$L_{S1}=19.17$ nH	$L'_{S1}=5.91$ nH	$R_{S1}=5$ Ohm	$C_{S2}=0.73$ fF
$L_{S2}=30.08$ nH	$L'_{S2}=4.29$ nH	$R_{S2}=10$ Ohm	$C_{S3}=1.363$ fF	$L_{S3}=14.48$ nH
$L'_{S3}=1.44$ nH	$R_{S3}=10$ Ohm	$C_{S4}=0.958$ fF	$L_{S4}=24.83$ nH	$L'_{S4}=10$ pH
$R_{S4}=10$ Ohm	$K_1=0.36$	$K_2=0.06$	$K_3=0.54$	$K_4=0.01$
$K_5=0.65$	$K_6=0.11$	$K_7=0.29$	$K_8=0.05$	

Table 2 The contrast of the transmission coefficient and the group delay

	Peak 1	Peak 2	Peak 3	Peak 4
The QL value of transmission coefficient	177.4	219.8	209.8	202.5
The QL value of group delay	399.1	412.1	479.3	491.8

\* loaded quality factor ( $Q_L = f_0 / (f_2 - f_1)$ ), where  $f_0$  is resonant frequency,  $f_1$  and  $f_2$  is the frequency that amplitude decreases to 0.707 times.

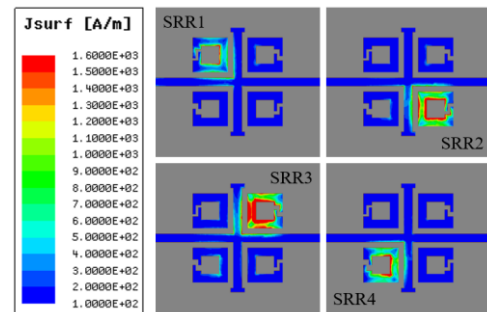


Fig. 3. Current distribution of the proposed sensor at 31.2GHz, 32.2GHz, 33.1GHz, 33.9GHz.

The features of structures with EIT-like effect can be used for the manufacturing of high-performance sensors. A polarization-independent metamaterial EIT sensor based on split ring resonators (SRRs) and spiral resonators (SRs) was proposed by Meng *et al.* for refractive index sensing with a sensitivity of 77.25 mm/RIU (Refract Index Unit) [23]. Lin *et al.* adopted fano resonance to an asymmetric periodical structure for compact double-functioning sensor excogitation [24]. Microstrip resonant coupling structures can also be devoted to engender EIT-like effect, which is more convenient for the integration as compared to periodical arrays. A straight-forward microstrip line structure is used to analog EIT-like effect with a sensitivity of 14.2mm/RIU [25], but the sensing is realized by the geometrical parameters variation of the SRRs.

In this paper, four SRRs with contiguous but independent resonate frequency as four bright mode resonator couple with two open stubs with the same dimension as one dark mode resonator. Each SRR couples with the metal DUT have different frequency response. SRRs have weak coupling with each other, with all of the four frequency response, the position of the crack and deformation can be defined with high precision.

The contributions of this paper are: 1) The sensing method

based on group delay using EIT-like effect is proposed with higher sensitivity; 2) The prototype of the sensor with dual sensing functions of the deformation sensing and crack sensing are designed and fabricated, which is useful in the structural health monitoring and 3) The working frequency is suggested in millimeter band to further increase the sensitivity.

## II. EIT-LIKE STRUCTURE DESIGN

The main sensing structure of the proposed sensor is based on multiband EIT-like effect. The open stub with a quarter wave length can be regarded as a “bright mode” resonator, which will generate a wide absorption band. The SRR with a half wave length is termed as “dark mode” resonator. When an SRR couples with the main microstrip line and the bright mode resonator, a narrow transmission window will appear in the wide stopband. To realize multiband EIT-like effect, four SRRs with different resonate frequency are distributed in four quadrants separated by main transmission line and two symmetric open stubs, as depicted in Fig. 1(a). The equivalent circuit of the proposed structure is shown in Fig. 1(b). The equivalent circuit can be derived from the EIT-like structure with only one open stub and one SRR. The open stub is equivalent to series RLC resonator, and the SRR is equivalent to an RLC series resonator. The coupling matrix of the multiband structure is complex, but the resonant frequencies of the SRRs are relatively distinguishable.

To further miniaturize the dimension of the proposed structure and reduce the influence of the different coupling length and distance between SRRs and the main transmission line as well as open stubs, two miniaturization methods are applied to open stubs and SRRs respectively. The open stub is shortened and separated at the tail. As for the SRR, its resonant frequency is influenced by the capacity value of the split and its resonate electric length. So, one conventional way of miniaturization is to add a cross finger capacitor at the crack of the ring [26]. The cross-finger capacitor has higher capacitive value than the capacitance that is produced by the gap of the SRR. So, the total size of the SRR is also reduced. The geometric parameters of the improved structure are shown in Fig. 1(a) as:  $w_M = w_S = 0.3$  mm,  $w_E = 0.15$  mm,  $w_C = w_G = 0.1$  mm,  $l_S = 1.24$  mm,  $l_C = 1.24$  mm,  $l_E = 0.5$  mm,  $d_M = d_E = 0.2$  mm,  $g_1 = 0.08$  mm,  $g_2 = 0.12$  mm,  $g_3 = 0.16$  mm,  $g_4 = 0.2$  mm. The structure is designed on Rogers 5880 substrate with the relative dielectric constant of 2.2 and the loss tangent of 0.0009. The thickness of the substrate is 0.254 mm.

The structure with slight modification to the substrate for measurement is simulated using high frequency electromagnetic simulation software ANSYS HFSS. The simulation and measured results are depicted in Fig. 2. The amplitude peak produced by simulation of each resonant frequency is the identical to the group delay peak. The current distribution of the four peaks (31.2GHz, 32.2GHz, 33.1GHz and 33.9GHz) is shown in Fig. 3. Each amplitude peak corresponds to one of the resonate frequency of the SRR. The SRR with larger capacitive value has lower resonant frequency. The simulated transmission peaks of the multiband sensor have different amplitude, which can be explained by the coupling matrix of the SRRs placed in different quadrants. Subsequently,

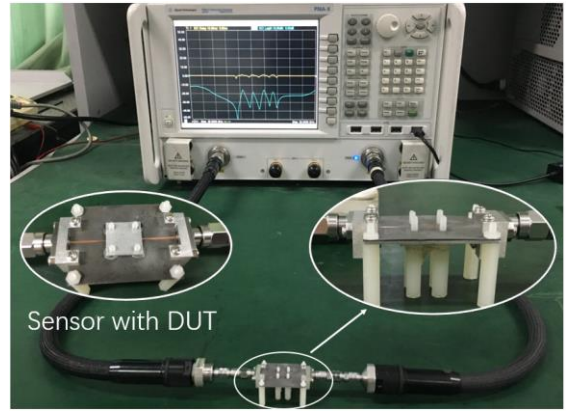


Fig. 4. Fabricated sensor and measurement setup

there is large transmission loss in the measurement caused by high frequency transmission loss (coaxial line and microstrip) and joint losses. As shown in the Fig. 2, the peaks of the group delay curve are sharper than the transmission curve. The contrast is listed in table 2. The quality factors of the group delay are larger than the transmission curve. Hence, group delay is a better sensing parameter than amplitude in the designed sensor. Here, the group delay sensing is refer to the shift frequency of group delay curve.

## III. THE SENSING CAPABILITY ANALYSIS

If the substrate material and upper dielectric medium are all fixed, resonant frequency of the SRR is decided by three factors: the total length of the ring, the capacitive value of the gap, and the width of the microstrip. For the designed multiband sensor, if a metal DUT is placed on top of the whole structure, all of the resonant frequency will be influenced. This property of the sensor can be used to detect the situation of the metal structure part, such as the deformation and crack.

### A. Deformation Sensing

The deformation of metal includes the change in its dimension and shape under presence external load and pressure. When the metal structure's parts especially the metal containers that are full of toxic or high temperature substances start aging, the probability of metal deformation caused by external force increases. Such type of substance's leakage might cause serious consequences. Therefore, it is crucial to detect the deformation position as soon as the aging of the metal structure parts starts and keep monitoring the deformation parts to determine the proper timing of maintenance and replacement.

The proposed multiband EIT-like sensor can detect the small shape change of the metal structure parts. A metal test block with a dimension of  $12 \times 12 \times 1$  mm is designed. The microstrip sensing structure fabricated on a substrate with the test block is simulated using ANSYS HFSS. According to the simulation results, the DUT must be close to the upper surface of the sensor, but no contact. The sensor can detect the change in shape within 1 mm. In fact, when the distance is more than 0.7 mm, no frequency shift is evident as compared to the sensor without the DUT. It has also been discovered that if the distances between the DUT and the SRRs are inconsistent, the frequency shift of each SRR is separated. Hence, the sensor can

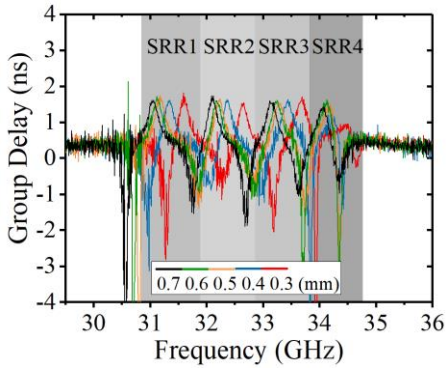


Fig. 5. Measurement results of group delay variation with the distance of DUT and sensor changing

detect the minute deformation in the area that the sensor structure covered. It implies that by utilizing further data processing techniques, the proposed sensor can precisely orientate the deformation.

### B. Crack Sensing

The cracks usually appear on the load-bearing structure parts as compared to the deformation of the metal structure parts, which indicates a more intuitive potential of serious damage and fracture of the structure. Undetected cracks due to fatigue or corrosion on metallic structures may cause hazardous incidents and therefore jeopardize human safety. There are several methods to detect crack including: nondestructive testing and evaluation (NDT&E) techniques, e.g., liquid penetrant testing, ultrasonic testing, eddy current testing, thermography testing, and microwave waveguide testing. The sensor proposed in this paper uses millimeter wave signal with a simple structure and possesses high sensitivity for its high-frequency characteristic.

When the DUT with crack is placed in front of the sensor, the coupling between the metal and sensor is changed. If the crack is located on the area that includes at least one SRR, the equivalent capacitance as shown in Fig. 1(b) will be changed, then the resonant frequency of this SRR is changed. The group delay peak shifting reflects the position of the crack.

## IV. EXPERIMENT SETUP AND RESULTS

The designed sensor is fabricated and test by Agilent N5244A Vector Network Analyzer (PNA-X). Fig. 4 depicts the measurement setup of sensor with and without DUT. Four plastic screws are fixed outside the sensor structure area for the orientation of the metal under test. The size of the sensor structure is about 5×5 mm, and the center of the screws are on the vertex of the square with 8mm on each edge. The radius of the screw hole is 2 mm. Several precise metal gaskets with 3 mm inner diameter and 5 mm outer diameter are used to change the distance between the sensor surface. The measured result is shown in Fig. 2. The measured transmission has lots of losses. These are caused by cable loss, joint loss and the transmission line loss because of high operating band, which is common in millimeter wave band. According to measured results, the group delay peaks are not decreased as much as compared to simulation except for slight frequency shift due to

manufacturing fault. It is an added advantage of using group delay as sensing parameter.

### A. The Variation of The Distance

As discussed and simulated in the previous section, the proper sensing distance between DUT and sensor is from 0.3 mm – 0.7 mm. It is validated by measurement as well. When the distance is less than 0.3 mm, the value of the group delay peak will decrease rapidly. The thickness of the precise gaskets is 0.2 mm and 0.3 mm respectively. Different distances are actualized by the combination of these two kinds of gaskets. Thus, the precision of the distances is not good enough but the errors are not large enough impact the variation of the four group delay peaks along with the distance. The result of group delay variation with the distance is depicted in Fig. 5. It is obvious that every SRR has a shifting area. When the DUT is placed on the sensor as shown in Fig. 4, the resonance frequency of the SRRs is shifted towards the higher frequency. The resonance frequency of SRR4 is outside of the stopband. Therefore, both the resonance frequency and the value of the group delay are changed. But the variation tendency of SRR4's group delay peak is similar to the other SRRs.

The measurement results of group delay variation with the distance are similar to the simulation results. This feature could be used for the orientation of the sensor. The sensor can be fixed with the metal under test (MUT) at first as the entire frequency shift stays the same with the measured value to make sure the sensor is placed strictly parallel with the MUT. Subsequently, when the MUT started to age, any change of the group delay represents the deformation or cracks of the MUT.

### B. Flipping the Metal DUT

When the metal deformed, there is inhomogeneity. The sensor can detect bulging process, and can further orientate the deformation part, by comparing the group delay with the standard balanced group delay. If the MUT is flipped to different direction, the equivalent capacitance between the MUT and the sensor changes as shown in Fig. 1(b), then the group delay result will be different. The measured results are depicted in Fig. 6. The reference group delay is chosen as 0.4 mm flat distance. One side of the MUT uses the gaskets with 0.2 mm thickness; the other side uses the gaskets with 0.6 mm thickness. As shown in Fig. 6(a), if the side close to SRR2 and SRR3 is 0.6 mm, consequently, the frequency of the group delay peak of SRR2 and SRR3 decreases. The same change can be observed in Fig. 6(b) and (d). In Fig. 6(c), the frequency change of SRR3 is due to an unexpected resonance in the frequency band between SRR2 and SRR3. The unexpected resonance might be introduced because the MUT is flipped to the direction of the input signal port. The measured results prove that after the balance procedure introduced before, the deformation of the MUT will be easily displayed by the variation of the group delay.

### C. Crack Sensing

The original metal crack usually has a width of 0.15 mm. To validate the crack sensing performance, a slot with a depth of



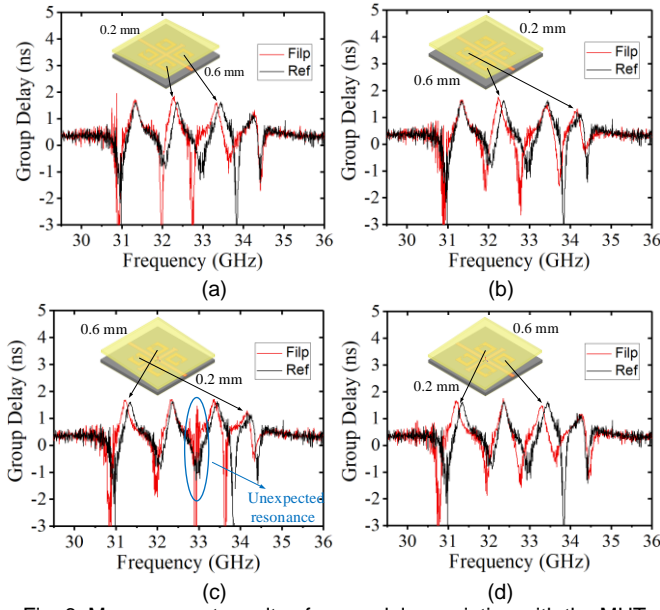


Fig. 6. Measurement results of group delay variation with the MUT flipping on different orientation.

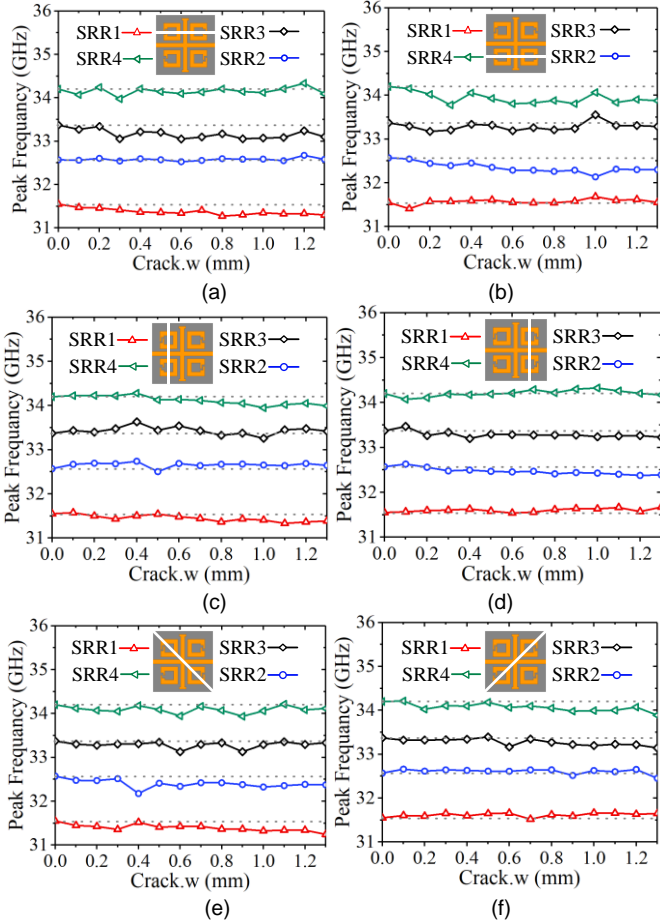


Fig. 7. Measurement results of the peak frequencies variation with different width of the slot on the MUT

0.2 mm is chamfered on the MUT with different position and direction. The width of the slot is tuned from 0.1 mm to 1.3 mm with the step of 0.1 mm, the measurement results are shown in Fig. 7. The distance between the MUT and the sensor is 0.4

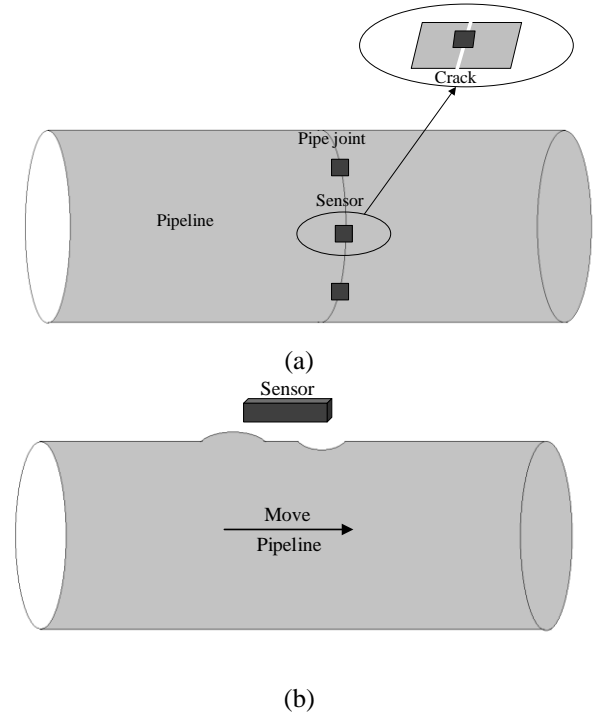


Fig. 8 Two kinds of application (a) permanent installation, (b) scanning application

mm. The white gap on the sensor area shows the position of the slot, and every figure shows the frequency variation of each SRR's group delay peak with the slot width. It is clear that the responses are different. The gray dot lines are the frequency of the SRRs without any crack on the MUT. For example, in Fig. 7(a), the slot is on SRR1 and SRR3, and the peak frequencies of which are under the gray line, while the frequencies of SRR2 and SRR4 remain as straight lines with the gray line. Similar responses can be observed on the other figures. The sensitivity  $s$  of the crack sensor with the MUT is defined and calculated as:

$$s = \frac{f_{wi} - f_{w0}}{wi} \quad (1)$$

where  $f_{w0}$  refer to the frequency of the SRRs without any crack on the MUT,  $f_{wi}$  ( $i = 1, 2, 3, \dots, 13$ ) refer to the frequency of the SRRs with crack on the MUT, and  $wi$  refer to the width of the slot. When the MUT is put on the sensor, the  $s$  can be calculated as  $s = 1.3\text{MHz}/\mu\text{m}$ .

#### D. Applications

The sensor is sensitive to the lift-off between the sensor and the MUT. when the height of the MUT is changed, the frequency of the sensor will shift. Two kinds of application are suggested and shown in Fig.8, (a) permanent installation, (b) scanning application. In real application, the sensing steps are listed as follows:

- 1) Install the MUT and sensor;
- 2) Measure the first group of data, and take it as the calibration data;
- 3) Measure the second group of data, and compared these two groups of data;
- 4) According to the difference of these two groups of data, the information of crack or deformation can be obtained.

In the industrial application, the fabrication tolerance is 0.01 mm, and the fabrication tolerance will affect the frequencies of SRRs. In this work, the detection of the sensor uses the relative value, so the fabrication tolerance will not affect the sensing.

## V. CONCLUSION

Based on previous work and the application of EIT-like effect, we proposed a group-delay-based sensor which can detect both the deformation and crack on the metal structure parts. The sensor has high precision and can further orientate the crack. The main structure of the proposed sensor is based on the concept of multi-band EIT effect. Multi-band EIT is actualized using serious of split-ring-resonators (SRR) coupling with each other to produce one wide stop band and four narrow pass band. The resonance frequencies of the SRRs are affected by the coupling amount variation between the SRRs and the part of metal device under test (DUT), which is placed close to the specific SRR. The orientation of metal deformation and crack is achieved by different frequency shifts of the four independent group delay peaks induced by multi-band EIT.

## ACKNOWLEDGMENT

This work was supported by in part by National Natural Science Foundation of China (NSFC) under Grant No. 61571084 and U1966201, and in part by the Fundamental Research Funds for the Central Universities (FRFCU) under Grant No. ZYGX2019Z022 and XGBDFZ03.

## REFERENCES

- [1] Y. Zhao, Y. N. Zhu, M. D. Yuan, J. F. Wang and S. Y. Zhu, "A laser-based fiber bragg grating ultrasonic sensing system for structural health monitoring," *IEEE Photon. Technol. Lett.*, vol. 28, no. 22, pp. 2573-2576, Nov, 2016.
- [2] J. Xu and H. K. Jo, "Development of high-sensitivity and low-cost electroluminescent strain sensor for structural health monitoring," *IEEE Sensors J.*, vol. 16, no. 7, pp. 1962-1968, Apr, 2016.
- [3] T. Chisholm, R. Lins and S. Givigi, "FPGA-based design for real-time crack detection based on particle filter," *IEEE Trans. Ind. Inform.*, 2019.
- [4] D. H. Wang and W. H. Liao, "Wireless transmission for health monitoring of large structures," *IEEE Trans. Instrum. Meas.*, vol. 55, no. 3, pp. 972-981, Jun, 2006.
- [5] K. Seoktae, "Development of millimeter wave integrated-circuit interferometric sensors for industrial sensing applications," *College Station, Tex.: Texas A & M University*, 2006.
- [6] Y. Zhao, Y. N. Zhu, M. D. Yuan, J. F. Wang and S. Y. Zhu, "Optimizing the Localization of a Wireless Sensor Network in Real Time Based on a Low-Cost Microcontroller," *IEEE Photon. Technol. Lett.*, vol. 28, no. 82, pp. 2573-2576, Nov.15, 2016.
- [7] B. S. Choi, J. W. Lee, J. J. Lee and K. T. Park, "A Hierarchical Algorithm for Indoor Mobile Robot Localization Using RFID Sensor Fusion," *IEEE Trans. Ind. Electron.*, vol. 58, no. 6, pp. 2226-2235, Jun, 2011.
- [8] G. J. Han, C. Y. Zhang, L. Shu and J. P. C. Joel, "Impacts of Deployment Strategies on Localization Performance in Underwater Acoustic Sensor Networks," *IEEE Trans. Ind. Electron.*, vol. 62, no. 3, pp. 1725-1733, Mar, 2015.
- [9] S. Jiang, L. Li, H. P. Xu, J. K. Xu, G. Y. Gu and S. B. Shull, "Stretchable e-Skin Patch for Gesture Recognition on the Back of the Hand," *IEEE Trans. Ind. Electron.*, vol. 67, no. 1, pp. 647-657, Jan, 2020.
- [10] M. H. Zarifi, D. Sameir, A. Mohammad, C. Bertie, R. Dennis, A. Michael, V. Nahid, H. Zaher, W. X. Chen and D. Mojgan, "A Microwave Ring Resonator Sensor for Early Detection of Breaches in Pipeline Coatings," *IEEE Trans. Ind. Electron.*, vol. 65, no. 2, pp. 1626-1635, Feb, 2018.
- [11] D. Sameir and D. Mojgan, "Multi -Resonant Chipless RFID Array System for Coating Detection and Corrosion Prediction," *IEEE Trans. Ind. Electron.*, 2019.
- [12] A. M. J. Marindra, G. Y. Tian, "Chipless RFID Sensor Tag for Metal Crack Detection and Characterization," *IEEE Trans. Microw. Theory Tech.*, vol. 66, no. 5, pp. 2452-2462, May, 2018.
- [13] D. A. Flavin, R. McBride and J. D. C. Jones, "Interferometric fiber-optic sensing based on the modulation of group delay and first order dispersion: application to strain-temperature measurand," *J. Lightwave Technol.*, vol. 13, no. 7, pp. 1314-1323, Jul, 1995.
- [14] Y. Lu, C. Baker, L. Chen and X. Bao, "Group-delay-based temperature sensing in linearly-chirped fiber bragg gratings using a kerr phase-interrogator," *J. Lightwave Technol.*, vol. 33, no. 2, pp. 381-385, Jan.15, 2015.
- [15] H. Hugo, H. Manfred, "A general relation for group delay and the relevance of group delay for refractometric sensing," *J. Opt. Soc. Am. B.*, vol. 31, no. 7, pp. 1561-1567, Jul, 2014.
- [16] R. S. Nair, E. Perret, S. Tedjini and T. Baron, "A group-delay-based chipless RFID humidity tag sensor using silicon nanowires," *IEEE Microw. Wireless Compon. Lett.*, vol. 12, pp. 729-732, 2013.
- [17] L. Zhang, P. Tassin, T. Koschny, C. Korte, S.M. Anlage and C.M. Soukoulis, "Large group delay in a microwave metamaterial analogue of electromagnetically induced transparency," *Appl. Phys. Lett.*, vol. 97, no. 24, pp. 633, 2013.
- [18] X. Q. Lin, J. W. Yu, Y. Jiang, J. Y. Jin and Y. Fan, "Electromagnetically induced transparencies in a closed waveguide with high efficiency and wide frequency band," *Appl. Phys. Lett.*, vol.101, no.9, pp. 093502, Aug, 2012.
- [19] J. Q. Gu, R. J. Singh, X. J. Liu, X. Q. Zhang, Y. F. Ma, S. Zhang, A. M. Stefan, Z. Tian, K. A. Abul, H. T. Chen, A. J. Talor, J. G. Han and W. L. Zhang, "Active control of electromagnetically induced transparency analogue in terahertz metamaterials," *Nat. Commun.*, vol. 3, pp. 1151, 2012.
- [20] H. Jung, C. In, H. Chio and H. Lee, "Electromagnetically Induced Transparency Analogue by Self-Complementary Terahertz Meta-Atom," *Adv. opt. mater.*, vol. 4, no. 4, pp. 627-633, 2016.
- [21] X. Q. Lin, J. Y. Jin, J. W. Yu, Y. Jiang, Y. Fan and Q. Xue, "Design and Analysis of EMIT Filter and Diplexer," *IEEE Trans. Ind. Electron.*, vol. 64, no. 4, pp. 3059-3066, 2017.
- [22] R. Singh, I. A. I. Alnaib, Y.P. Yang, C.D. Roy, W. Cao, C. Rockstuhl, T. Ozaki, R. Morandotti and W.L. Zhang, "Observing metamaterial induced transparency in individual Fano resonators with broken symmetry," *Appl. Phys. Lett.*, vol. 99, no. 20, pp. 201107, 2011.
- [23] F. Y. Meng, Q. Wu, D. Ermi, K. Wu and J. C. Lee, "Polarization-independent metamaterial analog of electromagnetically induced transparency for a refractive-index-based sensor," *IEEE Trans. Microw. Theory Techn.*, vol. 60, no. 10, pp. 3013-3022, Oct, 2012.
- [24] X. Q. Lin, Z. Chen, J. W. Yu, P. Q. Liu, P. F. Li and Z. Z. Chen, "An EIT-based compact microwave sensor with double sensing functions," *IEEE Sensors J.*, vol. 16, no. 2, pp. 293-298, Jan.15, 2016.
- [25] L. Zhu, J. H. Fu, F. Y. Meng, X. M. Ding, L. Dong and Q. Wu, "Detuned magnetic dipoles induced transparency in microstrip line for sensing," *IEEE Trans. on Mag.*, vol. 50, no. 1, pp. 1-4, Jan, 2014.
- [26] Y. X. Xiao, D. L. Su, S. Liu, "A Novel Compact Defected Ground Structure with Cross-Finger Gap," 2007 EMC, pp.358-360, Oct, 2007.



**Zhe Chen** was born in Hebei province, China, in April 1992. He received the B.S. degree in electromagnetic and wireless technology from the University of Electronic Science and Technology of China (UESTC), Chengdu, China, in 2015. He is currently working towards the Ph.D. degree in electromagnetic and microwave technology at UESTC.

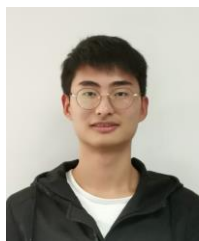


**Xian Qi Lin**(M'08-SM'15) was born in Zhejiang Province, China, on July 9, 1980. He received the B. S. degree in electronic engineering from the University of Electronic Science and Technology of China (UESTC), Chengdu, China, in 2003, and the Ph.D. degree in electromagnetic and microwave technology from Southeast University, Nanjing, China, in 2008. He joined the Department of Microwave Engineering, UESTC, in August, and became an Associate Professor and a Doctoral Supervisor in July 2009 and December 2011, respectively. From September 2011 to September 2012, he was a Postdoctoral Researcher in the Department of Electromagnetic Engineering, Royal Institute of Technology, Stockholm, Sweden. He is currently a Full Professor at UESTC. He has authored more than ten patents, more than 60 scientific journal papers, and has presented more than 60 conference papers. His research interests include microwave/millimeter-wave circuits, antennas, microwave power transmission and applications and.

biological effects, CubeSat antennas, Massive MIMO antenna arrays, UWB wind turbine blade deflection sensing, and RFID antennas.



**Yu Heng Yan** was born in Hebei province, China, in August 1996. He received the B.S. degree in electromagnetic and wireless technology from the University of Electronic Science and Technology of China (UESTC), Chengdu, China, in 2019. He is currently working towards the master degree in electromagnetic and microwave technology at UESTC.

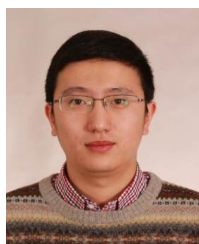


**Feng Xiao** was born in Sichuan province, China, in October 1995. He received the B.S. degree in electromagnetic and wireless technology from the University of Electronic Science and Technology of China (UESTC), Chengdu, China, in 2018. He is currently working towards the master degree in electromagnetic and microwave technology at UESTC.



(UESTC), Chengdu.

**Muhammad Talha Khan** was born in Karachi, Pakistan, in March 1986. He received BS degree in Electronics Engineering from Sir Syed University of Engineering and Technology (SSUET), Pakistan in 2010. He persuaded his MSc degree in Electrical & Electronics Engineering from Universiti Teknologi Petronas (UTP), Malaysia in October, 2015. He is currently persuading PhD degree in RF & Microwave Engineering at University of Electronic, Science and Technology of China



**Shuai Zhang** (SM'18) received the B.E. degree from the University of Electronic Science and Technology of China, Chengdu, China, in 2007 and the Ph.D. degree in electromagnetic engineering from the Royal Institute of Technology (KTH), Stockholm, Sweden, in 2013. After his Ph.D. studies, he was a Research Fellow at KTH. In April 2014, he joined Aalborg University, Denmark, where he currently works as Associate Professor. In 2010 and 2011, he was a Visiting Researcher at Lund University, Sweden and at Sony Mobile Communications AB, Sweden, respectively. He was also an external antenna specialist at Bang & Olufsen, Denmark from 2016-2017. He has coauthored over 50 articles in well-reputed international journals and over 16 (US or WO) patents. His current research interests include: mobile terminal mm wave antennas,